Research Article

Axial and torsional buckling analysis of single- and multi-walled carbon nanotubes: finite element comparison between armchair and zigzag types

Ramin Rahmani[1] · **Maksim Antonov**[1]

Abstract
The present work deals with the axial and torsional buckling analysis and design of carbon nanotubes (CNTs) by finite element. Computer-aided design, computer-aided engineering simulation, and finite element modeling are applied for the calculation of axial and torsional displacement and von Mises stresses. The smallest diameter of single-walled, double-walled, and multi-walled carbon nanotubes have been selected to survey armchair and zigzag types of CNTs. Nanotube diameters, covalent and van der Waals bonding, interlayer spacing, and chirality is considered in nanotubes construction based on actual dimensions. This paper illustrates that armchair-type nanotube is more resistant than zigzag-type against axial buckling for single-walled carbon nanotubes, whereas, in the case of torsional loading, zigzag-type show superior performance against buckling. By increasing the diameter and number of layers, due to van der Waals interaction, elastic buckling properties of nanotubes can be improved significantly. Data analysis for double-walled carbon nanotubes has shown that armchair-type is a better choice under combined loading, whereas, in the meantime, zigzag-type for triple-walled carbon nanotubes is preferred in the comparative analysis under combined loading. The results demonstrate the vital role of covalent intermolecular forces for single-walled nanotubes and van der Waals interlayer interactions for multi-walled nanotubes under buckling loading. The present study investigated the effect of covalent and van der Waals bonding for small diameter nanotubes.

Keywords Single- and multi-walled carbon nanotubes · Axial and torsional buckling · Armchair and zigzag types · Covalent intermolecular force · Van der Waals interlayer interaction · Finite element simulation

1 Introduction

During the last two decades, structural mechanics and properties, atomistic modeling, numerical and analytical simulation, prediction of carbon nanotubes (CNTs) behavior under different buckling loadings have been a major concern by investigators in the field of nanotechnology. Most famous classification of carbon nanomaterial in one molecule thickness is graphite sheets, nanotubes, nanocones, buckyball fullerenes that have attracted noticeable attention after their discovery and development [1, 2]. It is well illustrated in a variety of articles that single-walled and multi-walled carbon nanotubes (SWCNTs and MWCNTs) show excellent mechanical stability under combined loading including axial/torsional buckling and internal/external radial pressure [3, 4]. The mechanical characteristics of CNTs strictly depend on atomistic properties such as diameter, length, number of layers, chirality and helicity. Regarding structural configuration, there are three kinds of CNTs, namely, armchair, zigzag, and chiral that are tubular forms rolled up from graphite sheets [5, 6]. The electrical conductivity of SWCNTs is fully dependent on their chirality. Zigzag-type CNTs are semi-conductive due to energy gaps that prevent current flow, whereas armchair-type

✉ Ramin Rahmani, ramin.rahmaniahranjani@ttu.ee | [1]Department of Mechanical and Industrial Engineering, Tallinn University of Technology, Ehitajate Tee 5, 19086 Tallinn, Estonia.

SN Applied Sciences (2019) 1:1134 | https://doi.org/10.1007/s42452-019-1190-0

Received: 11 June 2019 / Accepted: 28 August 2019 / Published online: 31 August 2019

CNTs in the isolated tube (neither bundles nor multi-walled) are conductive [7]. Besides, CNTs have extraordinary thermal conductivity. Thermal loads and surrounding mediums are depending on buckling modes (longitudinal and circumferential wavenumbers) and aspect ratio (diameter to length proportion) [8].

Apart from theoretical and experimental investigations, three-dimensional finite element models (FEMs) as an analytical approach are helpful to predict the buckling behavior of nanotubes when subjected to combined loadings, Young's and shear modulus, von Mises stress and strain. Also, it can enable to compare displacement/dislocation in the armchair and zigzag types. Dependence of Young's modulus to CNT dimensions and chirality has been studied by FEM. Moreover, it has been shown that SWCNT chiral-type has higher Young's modulus than an armchair and zigzag [9]. A nonlocal elasticity shell simulation via ANSYS software has been presented to explain shell and column buckling and the correlation between length, thickness and radius ratios [10]. This FEM had excellent potential and coincidence with Donnell's stability equation to explain combined loadings and wave propagation in SWCNTs. Numerical study of vibrational properties (natural frequencies) for armchair and zigzag nanotubes [11], encapsulated symmetric (C_{60}) and asymmetric fullerenes(C_{70}) inside SWCNTs [12], chirality investigation of nanocones with different disclination angles [13], the effect of vacancy defects on Young's modulus and Poisson's ratio by finite element (FE) model [14] and bending buckling of nanotubes using molecular dynamic (MD) model [15] indicate the importance of modeling in nanotubes characterization.

The present research provides a new type of FEM analysis based on computer-aided design (CAD) and computer-aided engineering (CAE) using the software. This is the first study to anticipate axial/torsional buckling and covalent/van der Waals bonding behavior using CAD/CAE/FEM technique combined with rods-balls (atoms-bonds) model. Comparison between the armchair and zigzag types of single-walled, double-walled and triple-walled carbon nanotubes (SWCNTs, DWCNTs, and TWCNTs) is developed to figure out the best candidate for axial or torsional applications. In addition, the present paper aims to simulate the significance of covalent intermolecular forces and van der Waals interlayer interactions in SWCNTs and MWCNTs, in particular, in smallest diameter CNTs.

2 Atomic structure of CNTs

Armchair, zigzag and chiral types of SWCNTs are made by rolling a monoatomic graphene sheet into a cylinder. MWCNTs are multiple concentric rolled tubes embedded into each other. Due to covalent intermolecular bonding and van der Waals interlayer spacing, there is a geometrical restriction for smallest diameter of the armchair and zigzag types [16]. Armchair (2, 2) and Zigzag (4, 0) type SWCNTs are smallest diameter CNTs that include four carbon atoms in each row after rolling with diameters of approximately 3 Å. Configuration and geometrical dimensions of CNTs is shown in Fig. 1 and in Table 1. Curvature effect in small diameter of MWCNTs plays a crucial role, which is caused by interlayer van der Waals forces that are considered in the present paper [17]. Concentric nanotubes (2, 2) and (5, 5) embedded into each other and also (4, 0) and (9, 0) are built to provide smallest DWCNTs in an armchair and zigzag types, respectively. Therefore, based on Table 1, the smallest probable diameters of SWCNT, DWCNT and

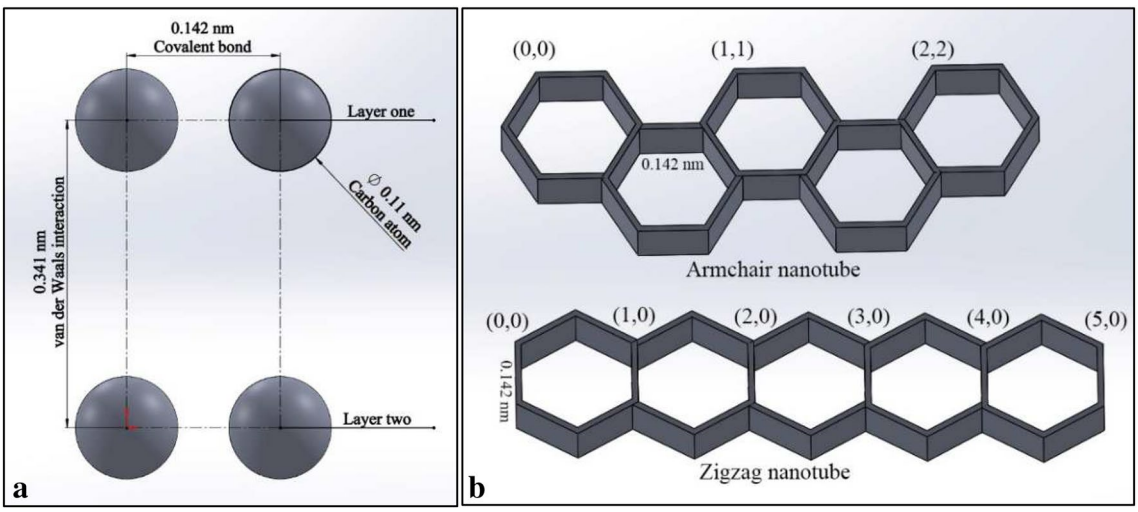

Fig. 1 Geometrical parameters for **a** atoms and layers spacing and **b** smallest diameter armchair and zigzag types

Table 1 Smallest diameter for providing SWCNT, DWCNT and TWCNT

CNTs type	Diameter (nm)	Length (nm)	Number of atoms
Armchair (2, 2)	0.271	0.861	32
Armchair (5, 5)	0.678	0.861	80
Armchair (8, 8)	1.085	0.861	128
Zigzag (4, 0)	0.313	1.136	48
Zigzag (9, 0)	0.705	1.136	108
Zigzag (14, 0)	1.096	1.136	168

TWCNT belong to armchair-type and are 0.271, 0.678 and 1.085 nm, respectively. Similarly, the smallest TWCNTs (as a MWCNTs) are made from the embedded armchair (2, 2), (5, 5) and (8, 8) into each other, and also zigzag (4, 0), (9, 0) and (14, 0) with almost 11 Å diameter. The diameter of the CNT is obtained as [18]:

$$\mathrm{D} = \frac{\mathrm{a}}{\pi}\sqrt{3\left(\mathrm{m}^2 + \mathrm{n}^2 + \mathrm{mn}\right)}, \quad 1.41\ \text{Å (graphite)} \le \mathrm{a} \le 1.44\ \text{Å (buckyball)} \tag{1}$$

where $a = 0.142$ nm is C–C bond length, (m, n) is chirality integers that for armchair CNTs is denoted by (m, m) and for armchair CNTs by $(n, 0)$. Then, smallest diameter for armchair (2, 2) is $\mathrm{D} = 3\mathrm{am}/\pi = 0.271\mathrm{nm}$ and for zigzag (4, 0) is $\mathrm{D} = \mathrm{am}\sqrt{3}/\pi = 0.313\mathrm{nm}$.

3 Analytical results and discussion

Three-dimensional finite element model of CAD/CAE/FEM, displacement of CNTs, and von Mises stress have been demonstrated for the various diameter of SWCNTs in Figs. 2 and 3 under axial and torsional loading according to data presented in Table 1. Accordingly, it is provided for DWCNTs and TWCNTs in Figs. 4 and 5, respectively. Fixed one-end in all models are assumed to define the boundary condition, while, the other is free subjected to axial or torsional loadings. 10 Pa pressure for axial loading and 1 N m torque for torsional loading is applied on top of each layer. Due to static analysis, changing the value of loading (pressure/torque/force) doesn't have influence in critical stress/displacement value. Covalent intermolecular bond distance, van der Waals interlayer length for adjacent nanotube layers, the diameter of a spherical carbon atom, honeycomb arrangement of the rolled graphene sheet, and configuration of smallest diameter armchair and zigzag types (based on Table 1, ~ 1 mm length for all types and ~ 0.3, ~ 0.7 and ~ 1 mm for single-, double- and triple-walled nanotubes, respectively), displacement and stress distribution are simulated based on experimental dimensions as a rod-ball model. According to our simulations, the buckling behavior has no clear dependence on the carbon nanotube length but governed by aspect ratio (proportion of diameter to length) [19]. The finite element simulation of the current research was carried out by SolidWorks X64 ©2016 and ANSYS workbench 17.2 ©2016 as individual designed ball-rod model and von Mises yield criterion that is expressed as [20]:

$$\sigma_{vonMises} = \sqrt{\frac{1}{2}\left[\left(\sigma_1 - \sigma_2\right)^2 + \left(\sigma_2 - \sigma_3\right)^2 + \left(\sigma_3 - \sigma_1\right)^2\right]} \tag{2}$$

where σ_1, σ_2 and σ_3 are the principal directions of the stress tensor.

As illustrated in Fig. 2, couple maximum of displacement and von Mises stress for SWCNT armchair (2, 2) is $\left(1.6 \times 10^{-2}\ \mathrm{nm}, 5.77 \times 10^{+7}\ \mathrm{Pa}\right)$, armchair (5, 5) is $\left(1.07 \times 10^{-5}\ \mathrm{nm}, 4.6 \times 10^{+4}\ \mathrm{Pa}\right)$, and armchair (8, 8) is $\left(8.2 \times 10^{-6}\ \mathrm{nm}, 4.05 \times 10^{+4}\ \mathrm{Pa}\right)$, respectively, and the upper part (atoms and bonds) of nanotube are affected significantly under axial loading. As well, as shown in Fig. 3, values of maximum displacement and maximum von Mises stress for SWCNT zigzag (4, 0) is $\left(1.71 \times 10^{-5}\ \mathrm{nm}, 4.8 \times 10^{+4}\ \mathrm{Pa}\right)$, zigzag (9, 0) is $\left(6.32 \times 10^{-6}\ \mathrm{nm}, 2.7 \times 10^{+4}\ \mathrm{Pa}\right)$, and zigzag (14, 0) is $\left(4.87 \times 10^{-6}\ \mathrm{nm}, 2.5 \times 10^{+4}\ \mathrm{Pa}\right)$ subjected to axial compressive load, respectively. The significant changes happen both in upper and middle parts. Numerical results reveal that armchair-type is more resistant than zigzag for axial compression and deformation. In the case of zigzag-type atomic structure, stress concentration from the upper part of SWCNTs is distributed toward middle and changes to wrinkling, whereas, for armchair-type, it remains in the top of SWCNTs just as buckling.

Figure 2 provides maximum of displacement and von Mises stress statistics of SWCNT under torsional loading that is $\left(4.5 \times 10^{-1}\ \mathrm{nm}, 5 \times 10^{+8}\ \mathrm{Pa}\right)$ for armchair (2, 2), $\left(1.52 \times 10^{-2}\ \mathrm{nm}, 5 \times 10^{+7}\ \mathrm{Pa}\right)$ for armchair (5, 5), and $\left(3.49 \times 10^{-3}\ \mathrm{nm}, 1.7 \times 10^{+8}\ \mathrm{Pa}\right)$ for armchair (8, 8), respectively. Critical stress, deformation and buckling rate of armchair-type nanotubes decreases significantly with the increase in the diameter of the nanotube. In addition, as illustrated in Fig. 3, maximum displacement and stress amount of SWCNT under torsional loading for zigzag (4, 0) is $\left(0.108\ \mathrm{nm}, 3.12 \times 10^{+8}\ \mathrm{Pa}\right)$, for zigzag (9, 0) is $\left(0.312\ \mathrm{nm}, 1.03 \times 10^{+9}\ \mathrm{Pa}\right)$, and for zigzag (14, 0) is $\left(0.2\ \mathrm{nm}, 7.14 \times 10^{+8}\ \mathrm{Pa}\right)$ subjected to torsional loading, respectively. These results show that zigzag-type CNTs are stronger under torsion than armchair. Data analysis display that displacement and stress during loading are first

progressive and then regressive. This finding is unexpected for zigzag-type that is not a fixed trend and it is independent of the diameter of SWCNTs surprisingly. Additionally, stress concentration is scattered in upper covalent bonds of zigzag-type CNTs. Overall, due to armchair-type atomic structure, stress is distributed in whole covalent bonds of SWCNT and make it more suitable than zigzag-type for torsional applications.

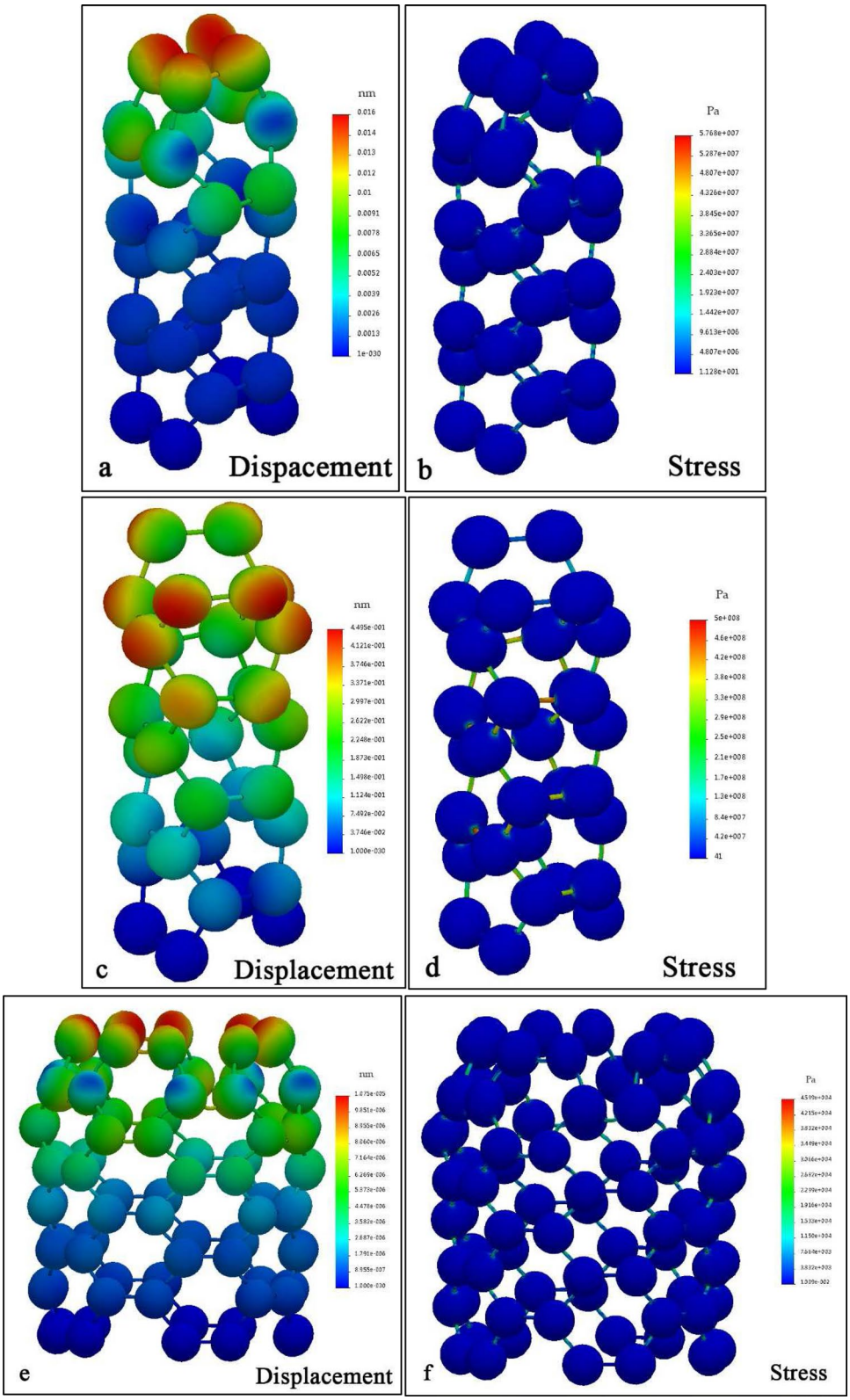

Fig. 2 Buckling analysis of armchair (2, 2) SWCNT **a** axial displacement, **b** axial stress, **c** torsional displacement and **d** torsional stress; Armchair (5, 5) SWCNT **e** axial displacement, **f** axial stress, **g** torsional displacement and **h** torsional stress; Armchair (8, 8) SWCNT **i** axial displacement, **j** axial stress, **k** torsional displacement and **l** torsional stress

Fig. 2 (continued)

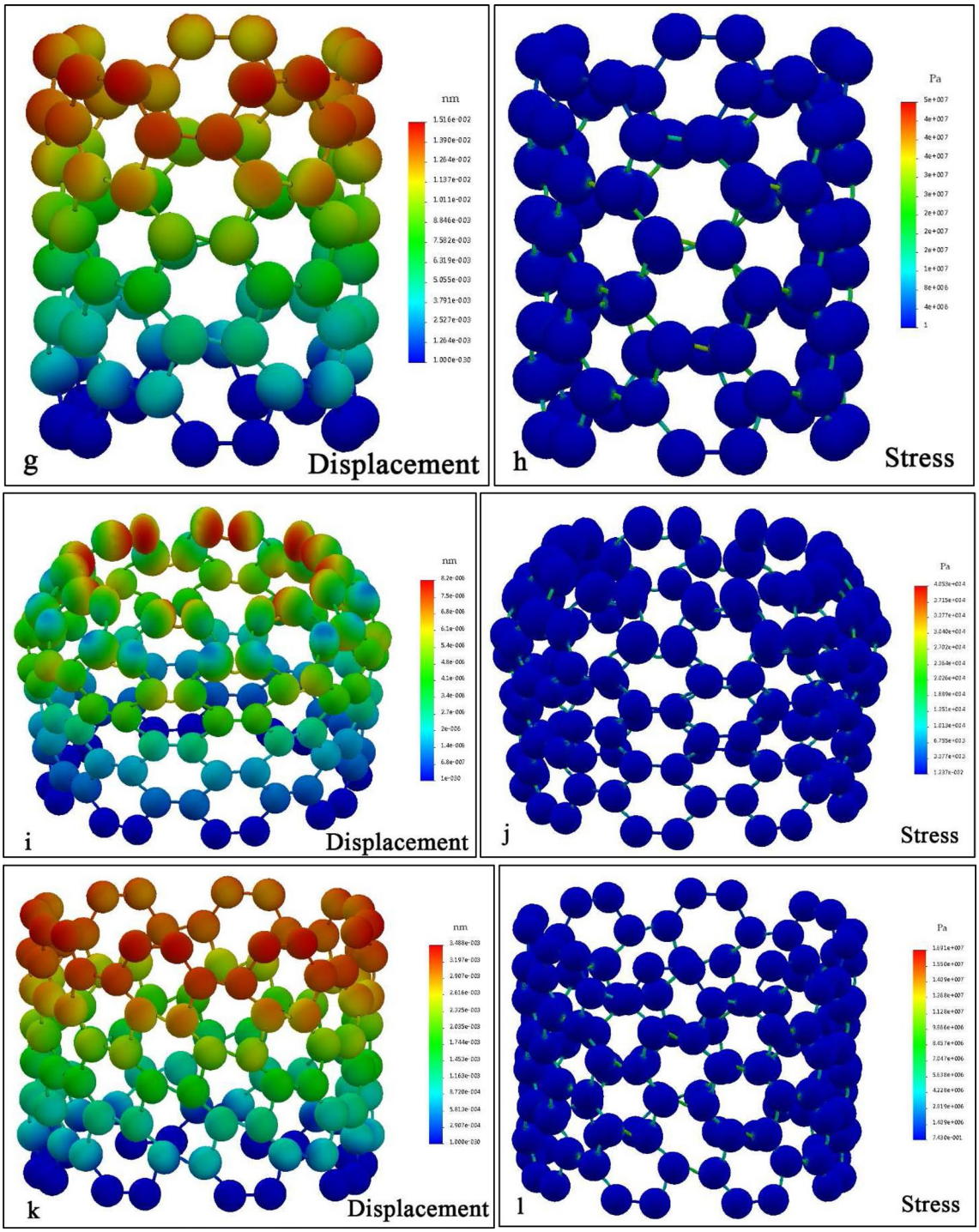

As can be seen from Figs. 4 and 5 for DWCNTs, the inner layer has more influence under compression, while, torsion somehow is tolerated by the outer layer. This phenomenon is more evident for zigzag-type DWCNT. Furthermore, it can be seen from Figs. 4 and 5 for TWCNTs that concentration of stress and displacement is reduced drastically from the innermost to the outermost layer. Displacement effect on carbon atoms, and stress on covalent and van der Waals bonding are well illustrated in a TWCNT as exhibited. Maximum displacement for DWCNT under axial and torsional loadings are 1.7×10^{-5} nm and 2.1×10^{-2} nm, respectively, that both amounts have occurred for zigzag-type. This is somewhat surprising that armchair-type DWCNT is a good choice for both kinds of loadings. On the other hand, 9×10^{-6} nm and 1.35×10^{-2} nm are maximum displacement values of TWCNT subjected axial and

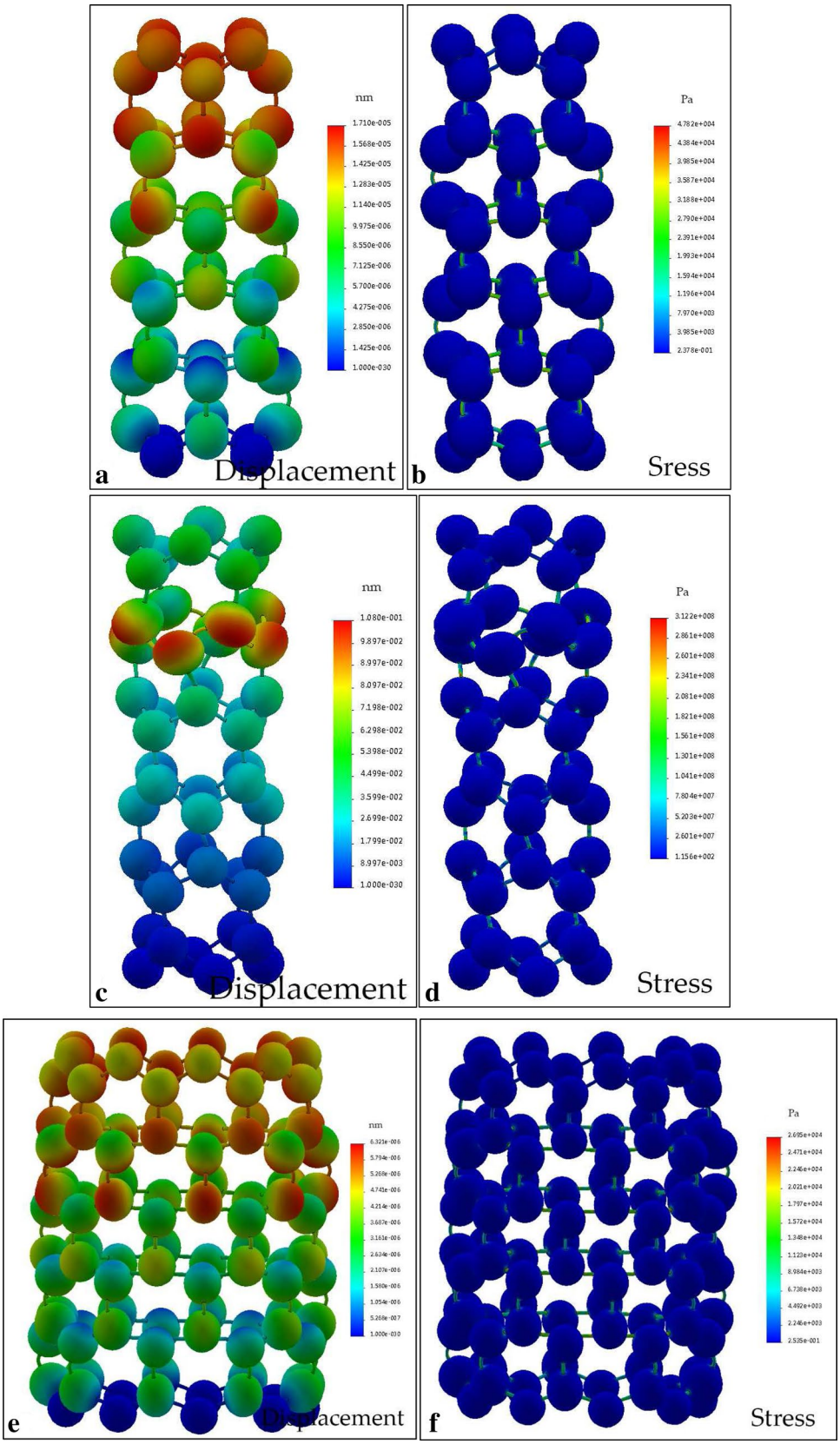

Fig. 3 Buckling analysis of zigzag (4, 0) SWCNT **a** axial displacement, **b** axial stress, **c** torsional displacement and **d** torsional stress; Zigzag (9, 0) SWCNT **e** axial displacement, **f** axial stress, **g** torsional displacement and **h** torsional stress; Zigzag (14, 0) SWCNT **i** axial displacement, **j** axial stress, **k** torsional displacement and **l** torsional stress

Fig. 3 (continued)

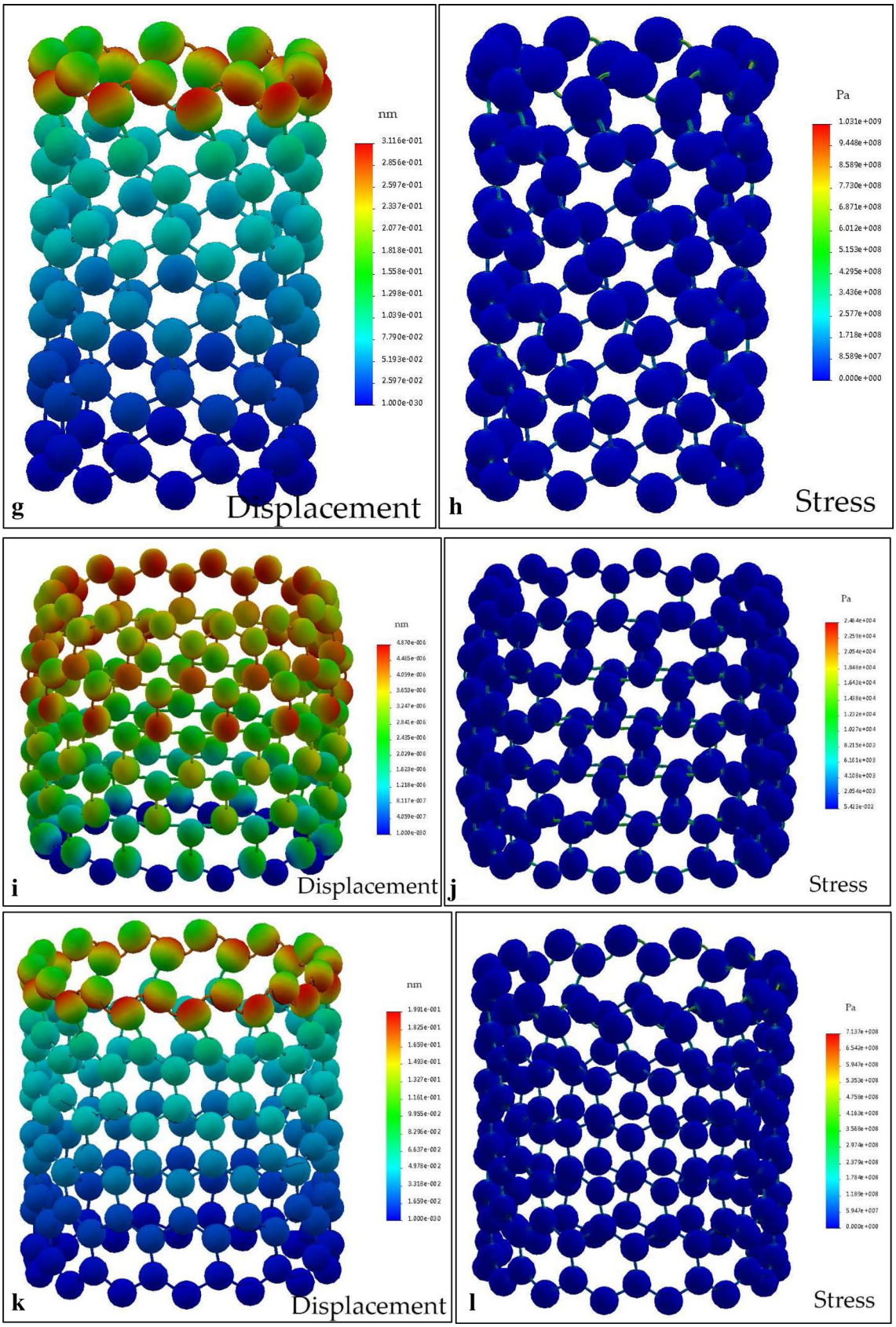

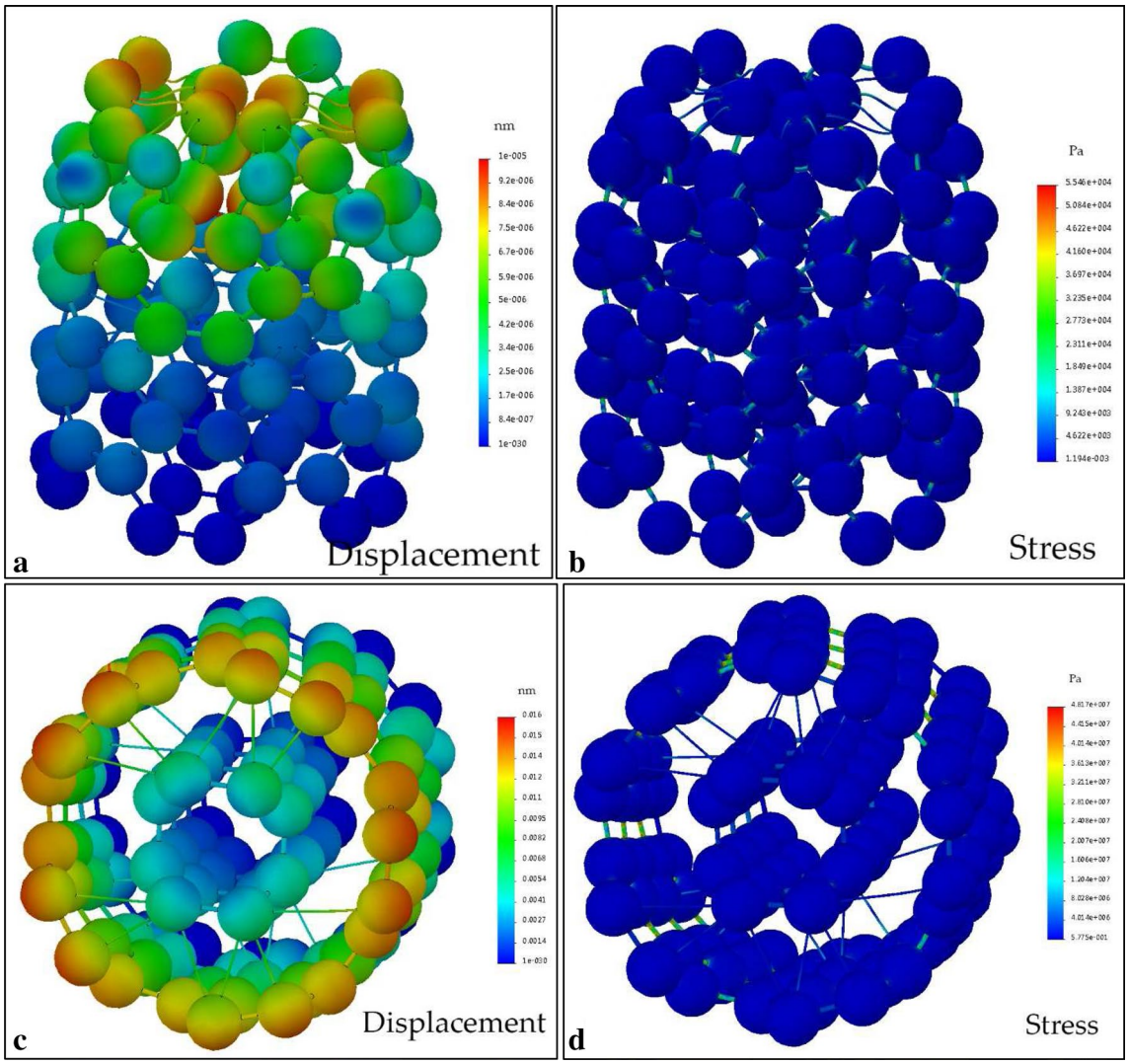

Fig. 4 Buckling analysis of armchair DWCNT **a** axial displacement, **b** axial stress, **c** torsional displacement and **d** torsional stress; Armchair TWCNT **e** axial displacement, **f** axial stress, **g** torsional displacement and **h** torsional stress

torsional loadings, respectively. For as much as both these amounts are recorded for armchair-type of TWCNT, it can be concluded that zigzag-type TWCNT and MWCNT is more resistant under combined loadings.

Maximum stress and displacement derived from Figs. 2, 3, 4 and 5 are given in Tables 2 and 3 for axial and torsional buckling, respectively. Based on Tables 2 and 3, an increase in load-bearing capacity and decrease in buckling rate has been occurred by either enhancement of layer diameter of SWCNT or number of layers of MWCNT. Data comparison of tables shows that armchair nanotubes are more resistant than zigzag when subjected to axial loading, whereas, in the case of torsional loading, zigzag-type show better performance. Maximum stress and distribution of stress of DWCNTs and TWCNTs under axial buckling (Table 2) are similar and this fact made DWCNT more favorable for axial reinforcement. On the other hand, TWCNTs due to van der Waals interactions, show stronger structures under torsional torques (Table 3). Comparison between Figs. 2k and 3k illustrate the weakness of zigzag-type with a bigger diameter under torsional loading. The software shows that fact by cracking in atoms, but in reality, separation on the bonds will happen. The increscent of layer numbers leads to an increase in stress concentration on bonds, not atoms. This concentration is more focused on van der Waals bonds for torsion (Figs. 4g, 5g), whereas, for axial, it is focused on covalent (Figs. 4e, 5e). Based on Figs. 4b, d and 5b, d for DWCNTs and Figs. 4f, h and 5f, h for TWCNTs, the outermost layer covalent bonds have to withstand the endurance of the nanotube structure under both kinds of loading (axial and torsion), whereas, declining MWCNTs start from vdW interaction in the innermost layer.

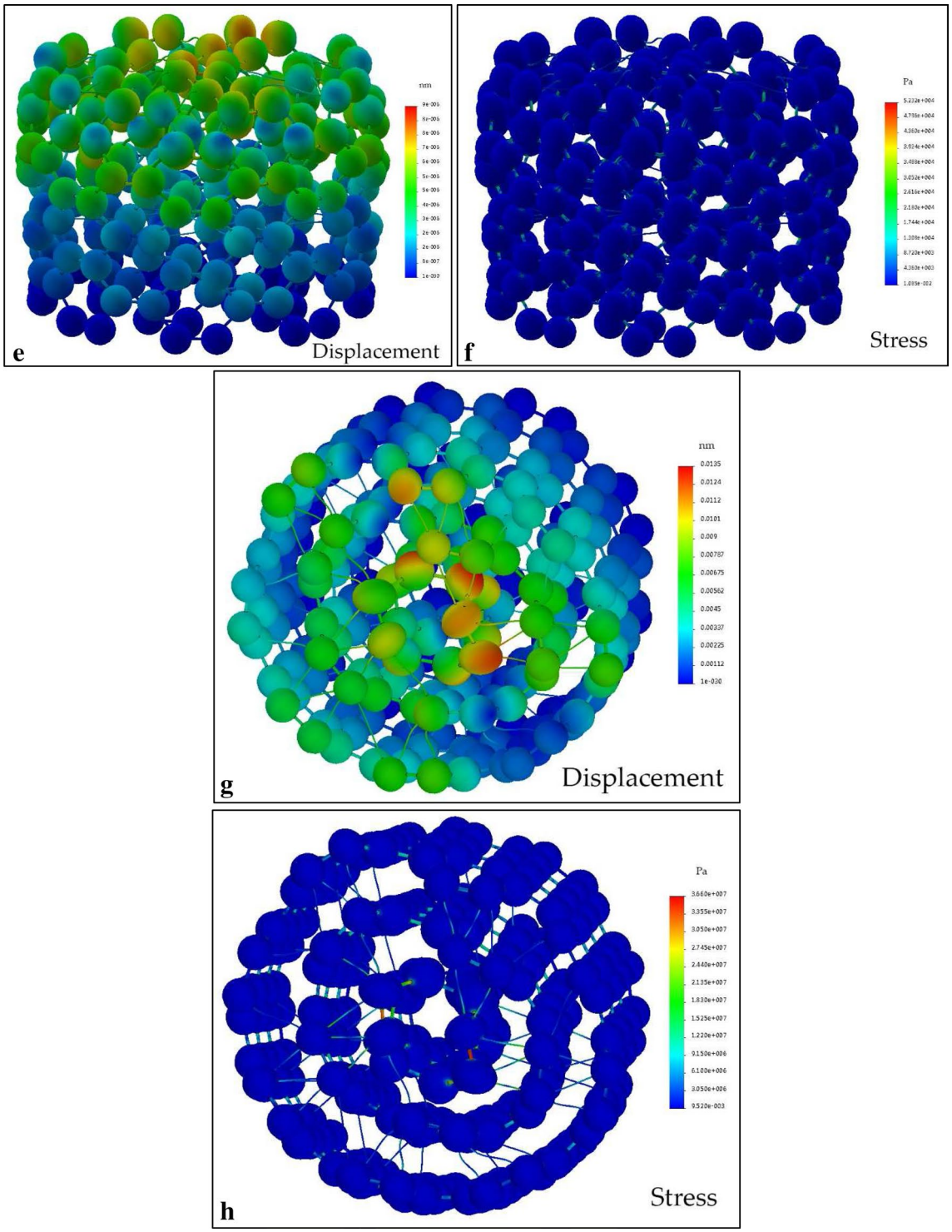

Fig. 4 (continued)

4 Conclusion

The findings of this study provide observation for application of suitable armchair or zigzag type of CNTs and buckling characteristic under axial pressure or bending torque. Regarding the diameter, analysis of smallest SWCNTs, DWCNTs, and TWCNTs (as MWCNTs) have shown that decrease in displacements, von Mises stress and buckling altogether with the increase in CNT diameter and layers (with same initial length).

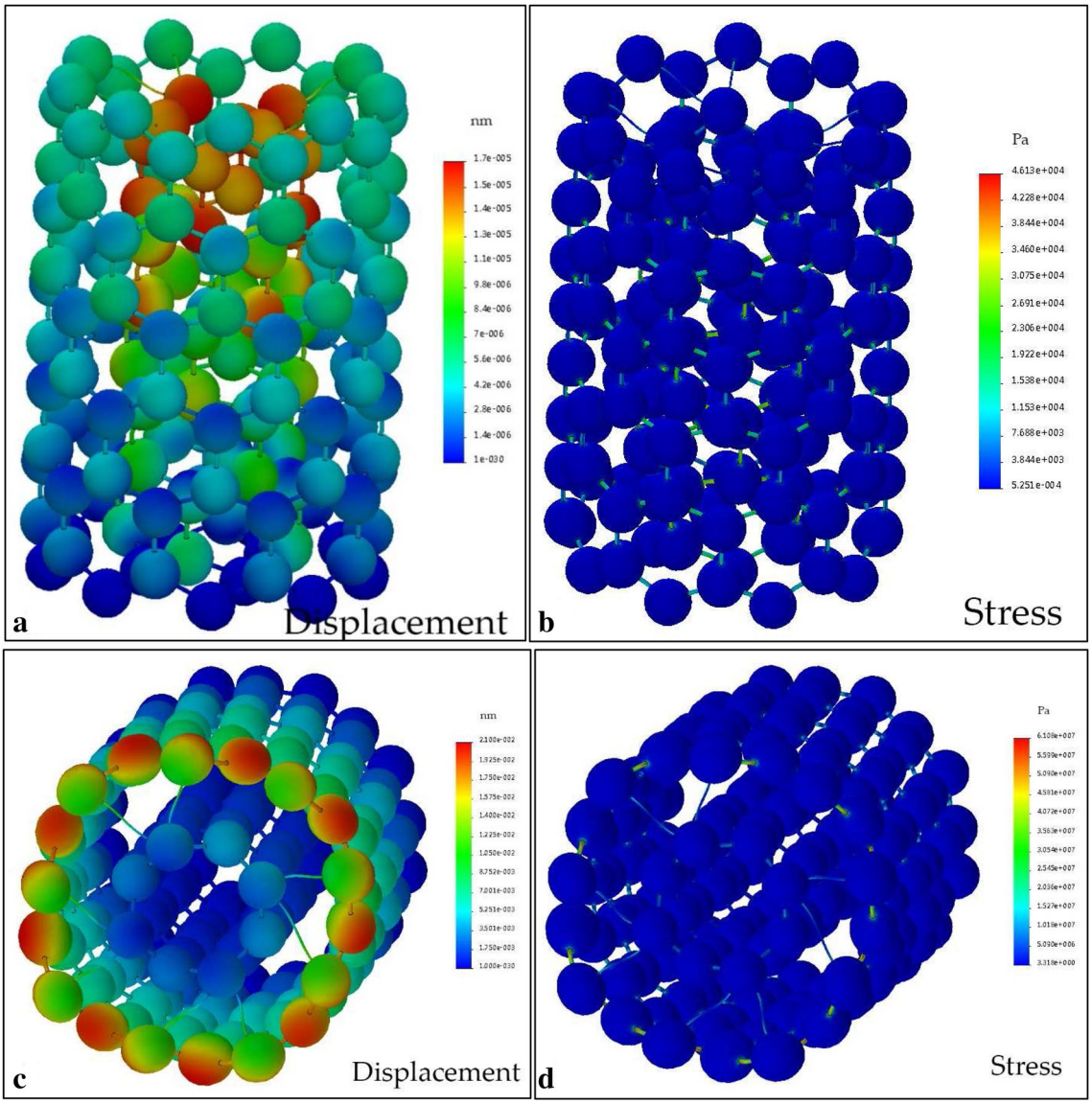

Fig. 5 Buckling analysis of zigzag DWCNT **a** axial displacement, **b** axial stress, **c** torsional displacement and **d** torsional stress; zigzag TWCNT **e** axial displacement, **f** axial stress, **g** torsional displacement and **h** torsional stress

The armchair-type SWCNTs exhibited good stabilization against axial buckling, whereas, the zigzag-type SWCNTs was a better choice under torsional buckling. Covalent intermolecular forces, van der Waals interlayer interactions, and carbon atoms are perfectly modeled by finite element rods and balls. In MWCNTs torsional buckling, covalent bonding has a more significant role, while van der Waals bonding is more important in axial buckling. For double-walled nanotubes, armchair-type has higher buckling resistance under axially compressed, torsional torque and/or combined loadings, whereas, zigzag-type is a better choice for triple- or multi-walled. This research is limited by the constant length of nanotubes but can be extended to any arbitrary length. In SWCNTs axial buckling, stress concentration occurs in the top of low diameter CNTs, that is progress toward the center by enhancement of diameter. If increasing of length was considered along with diameter increase, combined buckling and wrinkling investigation was needed.

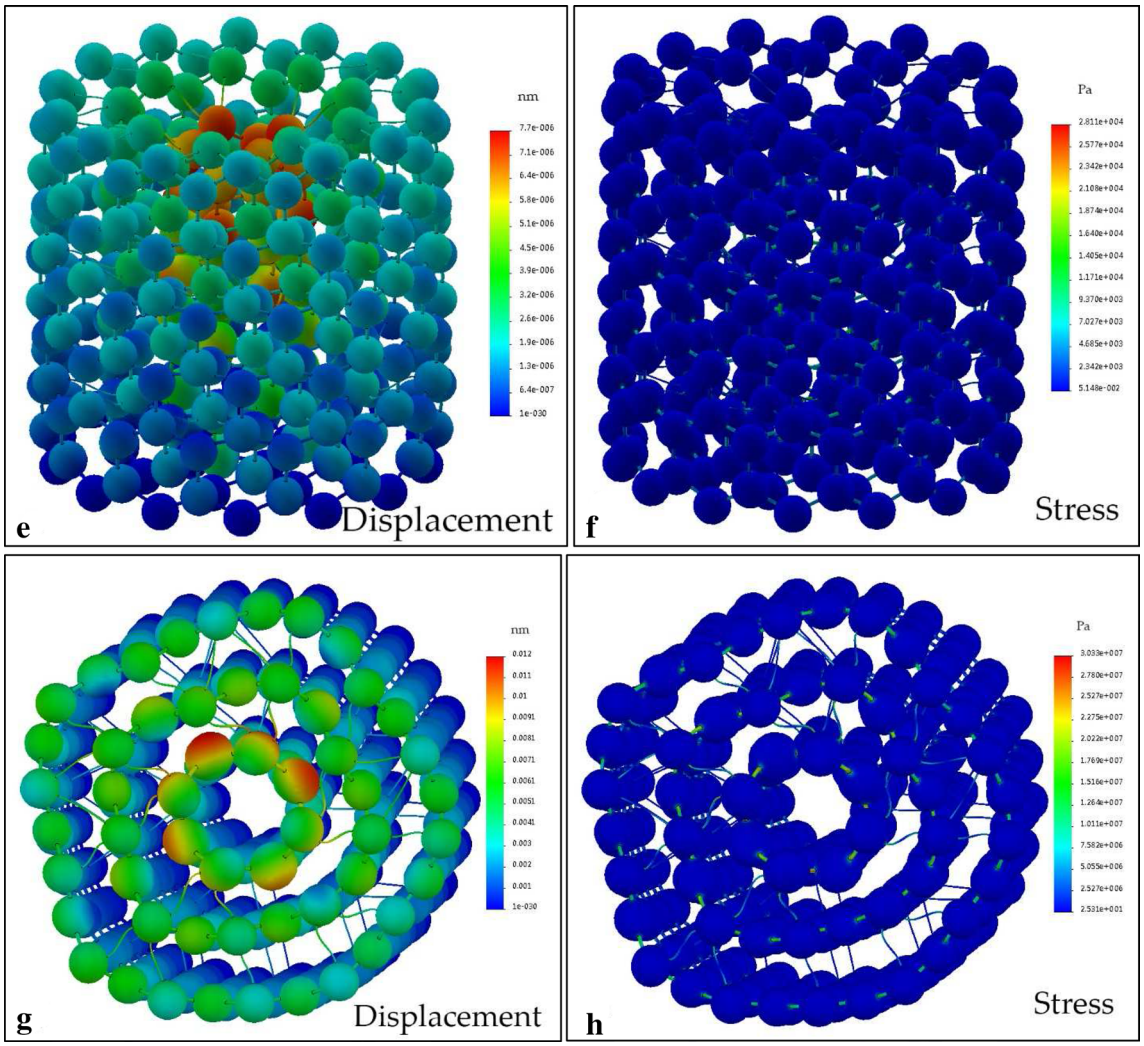

Fig. 5 (continued)

Table 2 Axial buckling finite element statistics of carbon nanotubes

Type	Layer	Maximum stress (kPa)	Maximum deformation (nm)
SWCNT	(2, 2)	577	1.60E−02
SWCNT	(5, 5)	46	1.07E−05
SWCNT	(8, 8)	40.5	8.20E−06
SWCNT	(4, 0)	47.8	1.71E−05
SWCNT	(9, 0)	27	6.32E−06
SWCNT	(14, 0)	24.6	4.87E−06
DWCNT	(5, 5) and (2, 2)	55.5	1.00E−05
DWCNT	(9, 0) and (4, 0)	46.1	1.70E−05
TWCNT	(8, 8), (5, 5) and (2, 2)	52.3	9.00E−06
TWCNT	(14, 0), (9, 0) and (4, 0)	28.1	7.70E−06

SWCNT single, *DWCNT* double, *TWCNT* triple walled carbon nanotubes

Table 3 Torsional buckling finite element statistics of carbon nanotubes

Type	Layer	Maximum stress (MPa)	Maximum deformation (nm)
SWCNT	(2, 2)	500	4.50E−01
SWCNT	(5, 5)	50	1.52E−02
SWCNT	(8, 8)	17	3.49E−03
SWCNT	(4, 0)	312	1.08E−01
SWCNT	(9, 0)	1030	3.12E−01
SWCNT	(14, 0)	714	2E−01
DWCNT	(5, 5) and (2, 2)	48.2	1.60E−02
DWCNT	(9, 0) and (4, 0)	61.1	2.10E−02
TWCNT	(8, 8), (5, 5) and (2, 2)	36.6	1.35E−02
TWCNT	(14, 0), (9, 0) and (4, 0)	30.3	1.20E−02

SWCNT single, *DWCNT* double, *TWCNT* triple walled carbon nanotubes

Compliance with ethical standards

Conflict of interest The authors declare that they have no conflict of interest.

Appendix

Single-walled carbon nanotubes armchair-type (2, 2), (5, 5) and (8, 8), zigzag-type (4, 0), (9, 0) and (14, 0), double-walled and triple-walled armchair has been shown as below:

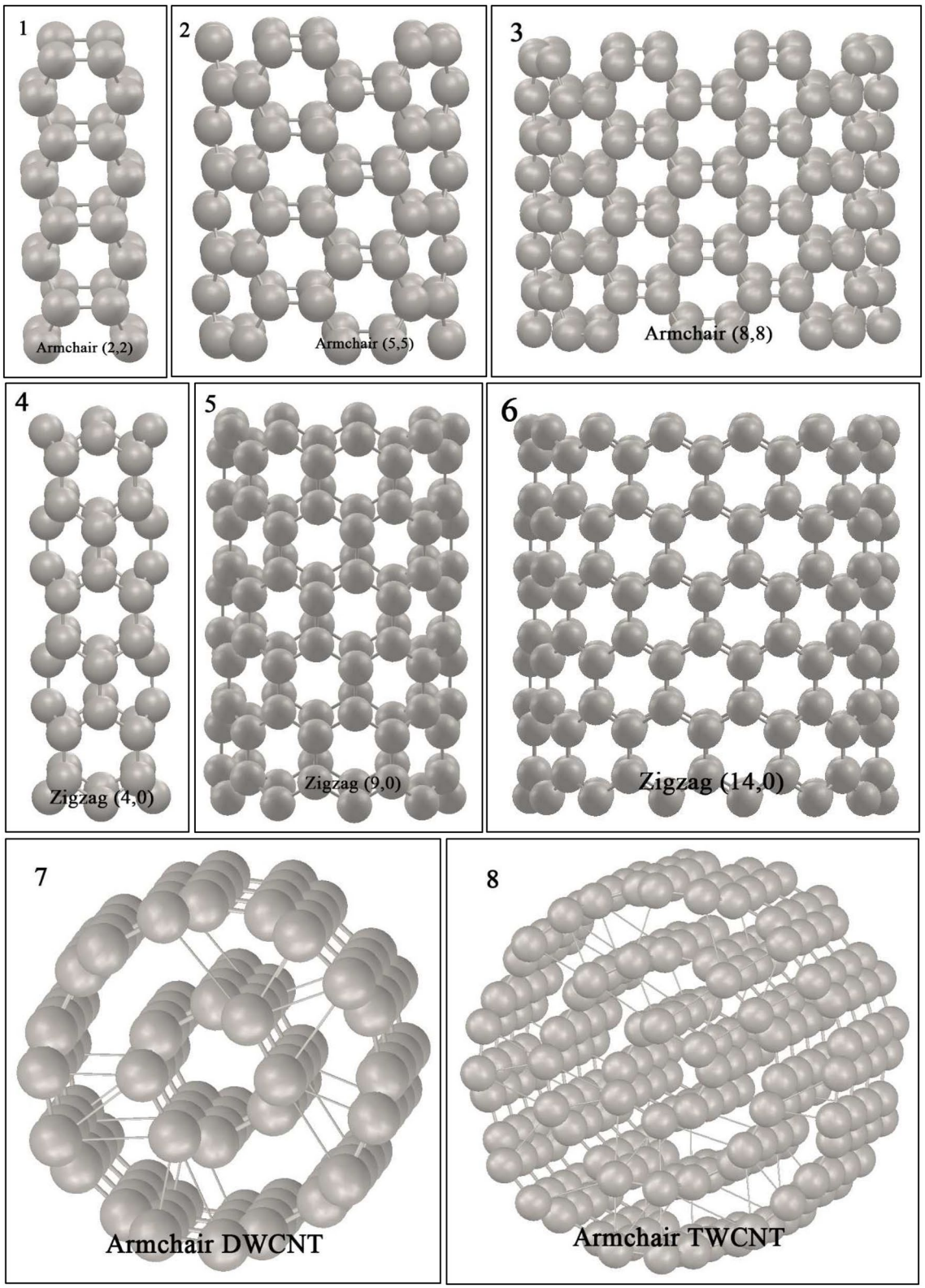

References

1. Iijima S (1991) Helical microtubules of graphitic carbon. Nature 354:56
2. Kroto HW, Heath JR, O'Brien SC, Curl RF, Smalley RE (1985) C60: buckminsterfullerene. Nature 318:162
3. Arani AG, Rahmani R, Arefmanesh A, Golabi S (2008) Buckling analysis of multi-walled carbon nanotubes under combined loading considering the effect of small length scale. J Mech Sci Technol 22:429
4. Sun C, Liu K (2008) Combined torsional buckling of multi-walled carbon nanotubes coupling with axial loading and radial pressures. Int J Solids Struct 45:2128
5. Li C, Chou TW (2003) A structural mechanics approach for the analysis of carbon nanotubes. Int J Solids Struct 40:2487
6. Thostenson E, Ren Z, Chou TW (2001) Advances in the science and technology of carbon nanotubes and their composites: a review. Compos Sci Technol 61:1899
7. Dresselhaus MS, Dresselhaus G, Eklund PC (1996) Science of fullerenes and carbon nanotubes. Academic Press, Cambridge
8. Yao X, Han Q (2007) The thermal effect on axially compressed buckling of a double-walled carbon nanotube. Eur J Mech A Solids 26:298
9. Tserpes KI, Papanikos P (2005) Finite element modeling of single-walled carbon nanotubes. Compos B 36:468
10. Arani AG, Rahmani R, Arefmanesh A (2008) Elastic buckling analysis of single-walled carbon nanotube under combined loading by using the ANSYS software. Physica E 40:2390
11. Mir M, Hosseini A, Majzoobi GH (2008) A numerical study of vibrational properties of single-walled carbon nanotubes. Comput Mater Sci 43:540–548
12. Troche KS, Coluci VR, Braga SF, Chinellato DD, Sato F, Legoas SB, Rurali R, Galvao DS (2005) Prediction of ordered phases of encapsulated C_{60}, C_{70}, and C_{78} inside carbon nanotubes. Nano Lett 5:349–355
13. Lee JH, Lee BS (2012) Modal analysis of carbon nanotubes and nanocones using FEM. Comput Mater Sci 51:30–42
14. Sakharova NA, Pereira AFG, Antunes JM, Fernandes JV (2016) Numerical simulation study of the elastic properties of single-walled carbon nanotubes containing vacancy defects. Compos B Eng 89:155–168
15. Cao G, Chen X (2006) Buckling of single-walled carbon nanotubes upon bending: molecular dynamics simulations and finite element method. Phys Rev B 73:155435
16. Zhao X, Liu Y, Inoue S, Suzuki T, Jones RO, Ando Y (2004) Smallest carbon nanotube is 3 Å in diameter. Phys Rev Lett 92(12):125502
17. Qian H, Xu KY, Ru CQ (2005) Curvature effects on axially compressed buckling of a small-diameter double-walled carbon nanotube. Int J Solids Struct 42:5426
18. Bhushan B (2010) Handbook of nanotechnology. Springer, Berlin
19. Wang X, Jiang Q, Xu W, Cai W, Inoue Y, Zhu Y (2013) Effect of carbon nanotube length on thermal, electrical and mechanical properties of CNT/bismaleimide composites. Carbon 53:145–152
20. Mises RV (1913) Mechanics of solid bodies in the plastically-deformable state. Klasse 4:582–592